PERGAMON

Journal of Quantitative Spectroscopy & Radiative Transfer 82 (2003) 363–382

Journal of Quantitative Spectroscopy & Radiative Transfer

www.elsevier.com/locate/jqsrt

The IR acetylene spectrum in HITRAN: update and new results

D. Jacquemart[a], J.-Y. Mandin[b], V. Dana[b], C. Claveau[b], J. Vander Auwera[c,1], M. Herman[c], L.S. Rothman[a,*], L. Régalia-Jarlot[d], A. Barbe[d]

[a] *Harvard-Smithsonian Center for Astrophysics, Atomic and Molecular Physics Division, 60 Garden Street, Cambridge, MA 02138-1516, USA*

[b] *Laboratoire de Physique Moléculaire et Applications, Université Pierre-et-Marie-Curie, CNRS, Case courrier 76, Tour 13, 4, place Jussieu, 75252 Paris Cedex 05, France*

[c] *Laboratoire de Chimie Physique Moléculaire C. P. 160/09, Université Libre de Bruxelles, 50, avenue F.D. Roosevelt, B-1050 Brussels, Belgium*

[d] *Groupe de Spectrométrie Moléculaire et Atmosphérique, Université de Reims-Champagne-Ardenne, CNRS, Moulin de la Housse, BP 347, 51062 Reims Cedex, France*

Received 9 December 2002; accepted 28 January 2003

Abstract

The 2000 HITRAN edition, with the updates of 2001, contains improved and new data on the acetylene molecule. The main changes concern the 13.6- and 7.5-μm spectral regions (improved line intensities), and the 5-μm region (previously absent from the database). These changes are reviewed, and the key problem of the validation of line intensities is dealt with. The status of the currently available line parameters is critically examined, and recommendations for future improvements are given.

Keywords: Acetylene; Infrared; Vibro-rotational transitions; Line parameters; Databases

1. Introduction

The infrared spectroscopy of the acetylene molecule C_2H_2 is important for atmospheric, planetary, astrophysical, and industrial applications. This molecule is present as a trace constituent in the upper atmosphere of the giant planets where it comes from methane photodissociation. Thus, the strong Q-branch of the ν_5 fundamental band, around 13.6 μm, was early on observed in the emission spectra

* Corresponding author. Tel.: +1-617-49-57474; fax: +1-617-49-67519.
E-mail address: lrothman@cfa.harvard.edu (L.S. Rothman).
[1] Research associate with the Fonds National de la Recherche Scientifique (FNRS, Belgium).

0022-4073/03/$ - see front matter
doi:10.1016/S0022-4073(03)00163-8

of the giant planets [1,2], and also of Titan, for example in those spectra recorded with the infrared radiometer-infrared spectrometer (IRIS) instrument on board Voyager 1 and 2 (see references cited in [3,4]). A few years ago, it was possible to deduce the stratospheric distribution of acetylene in Uranus from spectra obtained with the infrared space observatory (ISO) instrument [5]. Acetylene is also present in the terrestrial troposphere, where it is considered to be produced both by human activities [6] and some natural processes in seawater [7]. It is also present in the urban (see e.g. [8]) and industrial environment (see for example [9]) as a pollutant, with an increasing concentration since several years. In 1981, the first vertical profile of C_2H_2 was obtained from balloon flight spectra (Denver University) around 13.6 μm by Goldman et al. [10]. Finally, acetylene was observed in the circumstellar shell of cool carbon stars such as IRC+10216, and in interstellar clouds, through spectra recorded in the 3-μm region of the ν_3 fundamental band (see, e.g., [11,12] and references therein), and in the 13.6-μm region of the ν_5 fundamental band [13,14]. For these reasons, spectroscopic data concerning acetylene were introduced in the HITRAN database (molecule number 26) as early as the 1986 edition [15]. The two main 13.6- and 3-μm spectral regions of interest were represented, using the pioneering work of Varanasi et al. [3] and Rinsland et al. [11] for the line positions, Rinsland et al. [11] for the line intensities, Devi et al. [16] for the air-broadening coefficients, and Varanasi et al. [3,17] for the self-broadening coefficients and the temperature dependence of air-broadening coefficients. Some of these data are still present in the current issue of the database.

From another point of view, C_2H_2 is interesting for testing theoretical approaches. Detailed theoretical considerations on the acetylene molecule can be found in the book by Herman et al. [18], recently supplemented by statistical and dynamical interpretation [19]. Some of the data introduced in HITRAN since the 1986 edition resulted from improved measurements and modeling, by Hillman et al. [12] and Weber et al. [20–22], or by Vander Auwera et al. [23,24], taking into account vibro-rotational resonances both for energy levels and line intensities. Acetylene is also of interest for extending the global model of Perevalov et al. [25,26], initially adapted to the calculation of line positions and intensities of triatomic linear molecules such as CO_2 [27]. The measurement of a large amount of new line intensities in the 13.6- and 5-μm regions [28–31], together with already existing data in the 13.6- and 7.5-μm spectral regions [24,32], allowed the recently successful application of this model to the acetylene molecule [33]. Thus, because of their great theoretical interest, the numerous bands observed in the 5-μm region, previously absent in HITRAN, were introduced in the most recent edition.

The aim of this paper is to present the state of the HITRAN database concerning the acetylene molecule, to briefly review the recent work that has led to its improvement [24,28–31], and to give recommendations for future editions of HITRAN. Validation of data is one of the key problems that the management of databases has to deal with. This is the objective of a work initiated recently (at LPMA-Paris, and GSMA-Reims), involving measurements of line intensities for the numerous bands studied by Rinsland et al. [11] in the 3-μm region. The very first step of this study is to validate the line intensities of the two important ν_3 and $\nu_2+(\nu_4+\nu_5)^0_+$ cold bands observed in this region, and introduced in the previous HITRAN issue by Vander Auwera et al. [23]. The results of this validation will be presented in this paper.

The organization of the paper is as follows. In Section 2, the contents of HITRAN concerning C_2H_2 are recalled. Section 3 is devoted to the validation of line intensities, and to the first results of a work performed on the ν_3 and $\nu_2+(\nu_4+\nu_5)^0_+$ bands. Finally, in the conclusion, some recommendations are given for future editions of HITRAN.

2. The acetylene molecule in HITRAN

2.1. The acetylene molecule. Notations used to label levels and transitions

The acetylene molecule possesses numerous anharmonic resonances which give rise to a regular cluster structure [18,34–36] to the Hamiltonian matrix when an appropriate set of approximate constants of motion [37,38] is used. The eigenfrequencies ω_i of the acetylene molecule harmonic oscillators satisfy the following approximate relations

$$\omega_1 \approx \omega_3 \approx 5\omega_4 \approx 5\omega_5 \tag{1}$$

and

$$\omega_2 \approx 3\omega_4 \approx 3\omega_5, \tag{2}$$

so that vibrational levels can be gathered in polyads characterized by a given value of the pseudo-quantum number $P = 5v_1 + 3v_2 + 5v_3 + v_4 + v_5$, where v_1, v_2, v_3, v_4, and v_5 are the quantum numbers associated with the normal modes of vibration of the molecule (v_1 and v_3 are the symmetric and antisymmetric stretching modes respectively, v_2 is the CC stretch, and v_4 and v_5 are the *trans*- and *cis*-bending modes respectively). Following Perevalov et al. [25,26,33], it is convenient to name each polyad Pv_5, and in the same way, each spectral region ΔPv_5. With this notation, which we will adopt in the following, the spectral region nv_5 allows the study of upper levels belonging to the nv_5 polyad (through fundamentals and combination cold bands), to the $(n+1)v_5$ polyad (through hot bands arising from lower levels of the v_5 polyad), and so on.

In tables or in the HITRAN files, we followed the principles of Plíva [39,40] to label the vibrational levels. They are noted $v_1v_2v_3v_4v_5\ell \pm r$, with

$$\ell = |\ell_4 + \ell_5|, \tag{3}$$

ℓ_t being the vibrational angular momentum quantum number associated with the degenerate bending mode t, $\pm$ being the symmetry type for Σ vibrational states ($\ell = 0$), and r a roman numeral (or the corresponding digit in the HITRAN files) indicating the rank of the level, by decreasing energy value ($r = \mathrm{I}$ for the highest energy level), inside the set of states having the same vibrational symmetry, and coupled by ℓ-type resonances. When the two last indications are unnecessary, they are replaced by underscores ("_"); they are coded as blank spaces in the HITRAN files. As another notation more suited to the global fitting formalism exists, a table of correspondence is given in Ref. [33] to avoid ambiguities. In the assignment of vibro-rotational transitions, we have added the character e or f to the lower energy level.

Vibrational bands are labeled according to the following. For the upper level as for the lower one, when the two quantum numbers v_4 and v_5 are both different from zero, the notations v_4 and v_5 are put between parentheses, and only the true quantum number ℓ is mentioned. These notations are illustrated in Table 1. They suggest a self-explanatory and more spectroscopically comprehensive notation to use when a vibrational level is quoted in a text. For example, the upper level of the hot band $(2v_4 + 2v_5)^0_+\mathrm{II} - v_5^1$ will be labeled $000(22)^0_+\mathrm{II}$. For the sake of homogeneity, whatever the values of v_4, v_5, and ℓ are, one will use the notation $(v_4v_5)^\ell$. For example, the upper level of the hot band $v_2 + v_4^1 - v_5^1$ will be labeled $010(10)^1$. In Ref. [41], a table gives the correspondence between the eight-character ASCII representation adopted in HITRAN and the above spectroscopic notation.

Table 1
List of the acetylene bands present in HITRAN[a]

Band	v'	v''	Center	ν_{min}	ν_{max}	S_{min}	S_{max}	# lines	ΣS	J_{max}
$^{12}C_2H_2$										
$(\nu_4+\nu_5)^0_+$–ν_4^1	000110 + _	000101_	716.38[b]	604	841	2.9E−26	2.8E−20	149	5.9E−19	50
$2\nu_5^0$–ν_5^1	000020 + _	000011_	719.96[b]	606	843	9.5E−27	3.0E−20	150	6.8E−19	50
$(\nu_4+\nu_5)^0_-$–ν_4^1	000110 − _	000101_	728.87[b]	610	847	2.8E−26	3.2E−20	151	6.5E−19	50
$2\nu_5^2$–ν_5^1	000022_	000011_	729.15[b]	610	869	1.0E−26	3.2E−20	294	1.3E−18	50
ν_5^1	000011_	000000 + _	729.16[b]	611	848	8.4E−25	1.2E−18	150	2.5E−17	50
$(\nu_4+\nu_5)^2$–ν_4^1	000112_	000101_	731.12[b]	612	870	9.8E−27	3.1E−20	294	1.3E−18	50
$(\nu_4+\nu_5)^0_+$	000110 + _	000000 + _	1328.08[c]	1248	1415	2.6E−22	1.4E−19	71	2.7E−18	35
$\nu_2+\nu_4^1$–ν_5^1	010101_	000011_	1844.37[d]	1810	1899	5.7E−25	1.3E−23	74	4.3E−22	24
$(2\nu_4+2\nu_5)^0_+$II–ν_5^1	000220+	2000011_	1918.86[e]	1869	1979	1.7E−25	5.4E−24	60	1.1E−22	22
$(2\nu_4+2\nu_5)^0_-$–ν_5^1	000220 − _	000011_	1932.03[d]	1899	1966	4.6E−25	7.9E−24	51	1.4E−22	24
$(2\nu_4+2\nu_5)^2$II–ν_5^1	000222_	2000011_	1932.29[d]	1870	1991	1.8E−25	1.1E−23	48	1.6E−22	27
$(2\nu_4+\nu_5)^1$II	000211_	2000000 + _	1940.00[d]	1860	2011	3.8E−25	2.5E−22	97	5.1E−21	34
$(3\nu_4+\nu_5)^2$II–ν_4^1	000312_	2000101_	1945.13[d]	1883	2006	4.3E−25	2.8E−23	142	1.0E−21	27
$(3\nu_4+\nu_5)^0_+$–ν_4^1	000310 + _	000101_	1948.91[e]	1915	2008	1.8E−24	3.0E−23	52	5.3E−22	23
$(2\nu_4+\nu_5)^1$I	000211_	1000000 + _	1959.70[d]	1897	2025	6.0E−25	6.4E−23	81	1.3E−21	28
$(3\nu_4+\nu_5)^0_-$–ν_4^1	000310 − _	000101_	1972.15[d]	1948	1999	1.9E−25	7.6E−24	43	1.0E−22	23
$(3\nu_4+\nu_5)^2$I–ν_4^1	000312_	1000101_	1973.28[e]	1943	2003	7.5E−26	4.0E−24	63	9.8E−23	13
$\nu_2+\nu_5^1$–ν_4^1	010011_	000101_	2090.21[d]	2038	2140	5.5E−25	6.6E−24	79	2.4E−22	21
$(\nu_4+3\nu_5)^0_+$–ν_4^1	000130 + _	000101_	2146.10[d]	2101	2199	4.3E−25	6.8E−24	58	1.4E−22	20
$4\nu_5^0-\nu_5^1$	000040 + _	000011_	2151.07[d]	2089	2224	4.1E−25	2.0E−23	80	4.6E−22	28
$(\nu_4+3\nu_5)^2$II–ν_4^1	000132_	2000101_	2156.79[e]	2111	2215	9.8E−26	6.1E−24	119	2.0E−22	21
$4\nu_5^2$–ν_5^1	000042_	000011_	2160.21[e]	2103	2222	1.6E−25	1.9E−23	140	6.9E−22	27
$3\nu_5^1$	000031_	000000 + _	2169.17[d]	2088	2255	4.1E−25	3.9E−22	105	8.0E−21	35
$(\nu_4+3\nu_5)^0_-$–ν_4^1	000130 − _	000101_	2171.96[d]	2112	2233	2.3E−25	1.1E−23	75	2.5E−22	26
$(\nu_4+3\nu_5)^2$I–ν_4^1	000132_	1000101_	2179.10[e]	2129	2236	1.0E−25	6.3E−24	128	2.2E−22	27
$\nu_2+(\nu_4+\nu_5)^0_+$	010110 + _	000000 + _	3281.90[f]	3204	3352	2.2E−21	2.5E−19	63	5.0E−18	31
ν_3	001000 + _	000000 + _	3294.84[f]	3211	3359	8.9E−22	2.2E−19	62	4.4E−18	33
$^{12}C^{13}CH_2$										
ν_5^1	000011_	000000 + _	728.23[g]	613	844	3.8E−26	1.6E−20	150	4.9E−19	50
ν_3	001000 + _	000000 + _	3284.19[h]	3178	3375	1.2E−24	6.2E−21	86	1.8E−19	43

[a]Bands and energy levels are noted as explained in text (Section 2.1). In the HITRAN files, underscores ("_") are replaced by blank spaces. Approximate values of band centers and wavenumbers (ν) are in cm^{-1}. Line intensities (S) are in units of $cm^{-1}/(molecule\ cm^{-2})$ at 296 K, in natural abundances (97.760% of $^{12}C_2H_2$ and 2.197% of $^{12}C^{13}CH_2$). ΣS is the sum of the intensities of the lines present in HITRAN for the concerned band. Other notations are self-explanatory. References for band centers are the following:

[b]Kabbadj et al. [54].
[c]Vander Auwera [24].
[d]Plíva [39].
[e]From empirical polynomial fits of experimental line positions of Refs. [31,39].
[f]Vander Auwera et al. [23].
[g]Di Lonardo et al. [44].
[h]Rinsland et al. [11].

2.2. Review of bibliography about experimental data in the IR and origin of the HITRAN data

Before describing the HITRAN data, we present some bibliographic information.

An extensive bibliography on the acetylene molecule can be found in the book by Herman et al. [18], especially concerning line assignments and vibrational levels (energy level values up to about 24,000 cm^{-1}), recently supplemented by an extensive review on the vibrational energy states in the ground electronic state of three isotopomers of acetylene: $^{12}C_2H_2$, $^{12}C_2D_2$ and $^{13}C_2H_2$ [42]. Among recent work, one should note the study of Vander Auwera et al. [43], in which more than 600 absolute line positions of $^{12}C_2H_2$ were measured for 11 bands, between 7060 and 9880 cm^{-1}. Also of note are the numerous results of Di Lonardo et al. [44], concerning 5300 vibro-rotational transitions, for 53 bands of the $^{12}C^{13}CH_2$ isotopic species, between 450 and 3200 cm^{-1}.

In Table 1 of [28], references concerning $^{12}C_2H_2$ experimental band or line intensities have been gathered, for the IR and visible spectral domains. To update this list, one should add the following work concerning the main isotopic species:

- Herregodts et al. [45]: individual line intensities in the $\nu_1 + 3\nu_3$ band (around 12680 cm^{-1}). Very recent Fourier transform spectroscopy measurements show that these intensities are significantly too low [46].
- Vander Auwera [24]: individual line intensities in the $\nu_4 + \nu_5$ band (around 1330 cm^{-1}); note that these results were put in the 2000 HITRAN edition.
- El Hachtouki and Vander Auwera [47]: individual line intensities in the $\nu_1+\nu_3$, $\nu_1+\nu_2+(\nu_4+\nu_5)^0_+$, $\nu_1 + \nu_3 + \nu_4 - \nu_4$, and $\nu_1 + \nu_3 + \nu_5 - \nu_5$ bands (around 6500 cm^{-1}). Note that line intensities were also obtained for the $\nu_1 + \nu_3$ band of $^{12}C^{13}CH_2$ in that work.

Similarly, in Table 1 of Ref. [30], some references about pressure effects on $^{12}C_2H_2$ lines had been given. Corrections and updates concerning the main isotopic species are the following:

- The work of Pine and Looney [48] and of Pine [49] (unfortunately overlooked) must be added. They concerned line-mixing studies in the $\nu_1+\nu_5$, $\nu_3+\nu_4$, and $\nu_2+2\nu_4+\nu_5$ bands around 4000 cm^{-1} (buffer gas: C_2H_2) [48], and collisional broadening, shifting, and narrowing coefficients, as well as line-mixing parameters, in the $\nu_1 + \nu_5$ band around 4000 cm^{-1} (buffer gas: C_2H_2, N_2, or Ar) [49].
- The recent work of Blanquet et al. [50] has to be taken into account: line mixing (buffer gas: He or N_2) for two hot bands around 720 cm^{-1}, at 173, 183, and 198 K.

Starting from the 1986 HITRAN edition, the contents of the next issues, concerning the two isotopic species $^{12}C_2H_2$ and $^{12}C^{13}CH_2$, were improved as follows:

- In the 1991 and 1992 issues [51], data are present, for the main isotopic species, at 13.6, 7.5, and 3 μm; data on $^{12}C^{13}CH_2$ are present only at 3 μm.
- In the 1996 issue [32], the database was noticeably updated and improved. At 13.6 μm, line positions and intensities were replaced with the values issued from the work of Hillman et al. [12] and Weber et al. [20–22], for the ν_5 band and five hot bands of $^{12}C_2H_2$, and the ν_5 band of $^{12}C^{13}CH_2$ was added. At 3 μm, the line positions and intensities of Vander Auwera et al. [23] were used to update the database.

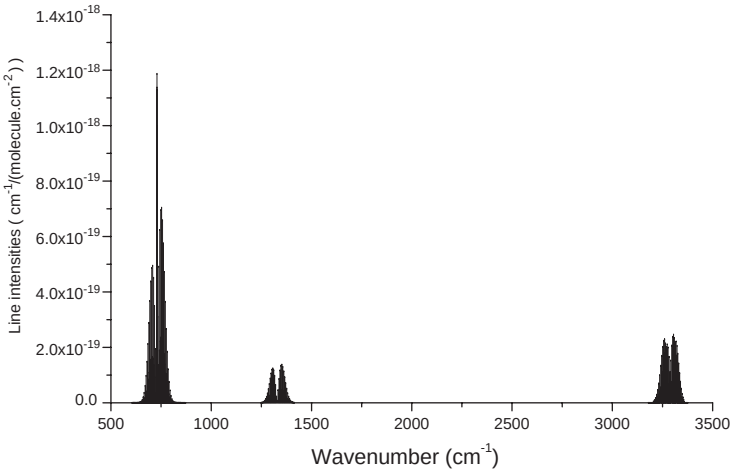

Fig. 1. Synthetic spectrum of the main isotopic species of acetylene between 500 and 3500 cm^{-1}. This spectrum, computed using the 2000 HITRAN data, shows the strongest bands in the ν_5, $2\nu_5$, and $5\nu_5$ spectral regions.

Let us recall that empirical expressions, vs. the running index $|m|$, from the work of Devi et al. [16], were used to calculate the air-broadening coefficients, and that the expression reported by Varanasi et al. [3,17] was used to calculate the self-broadening coefficients. The temperature dependence of the air-broadening coefficients is from Varanasi et al. [3,17]. However, no air-pressure shifts were reported.

2.3. The 2000 HITRAN edition plus updates of 2001

Table 1 is a summary of the acetylene bands present in the HITRAN database [41]. Synthetic spectra of the main isotopomer have been computed from these data, and plotted in Figs. 1 and 2. Only two bands of the $^{12}C^{13}CH_2$ isotopic species are present in HITRAN: the ν_5 band at 13.6 μm, and the ν_3 band at 3 μm. As far as $^{12}C_2H_2$ is concerned, one finds the following data.

2.3.1. The 13.6-μm spectral region

In this region (the ν_5 spectral region between 604 and 870 cm^{-1}), the database contains an extensive set of transitions for the ν_5 band and five hot bands. The original HITRAN data came mainly from the experimental and theoretical work of Hillman et al. [12] and Weber et al. [20–22] concerning energy levels, line positions and intensities. Improved line intensities have been introduced for the 2000 HITRAN edition from the work of Mandin et al. [28] and Jacquemart et al. [29]. Details about the changes vs. the 1996 issue are given in Ref. [29]: only line intensities and transition dipole moment squared values were modified. They have been calculated using Herman–Wallis coefficients deduced from experimental results, so that resonances were not explicitly taken into account. Moreover, the symmetry character e or f of the lower level was systematically added. This attribution was missing in the previous issue [32], so that in the case of bands with ℓ-type doubling, and for the two hot bands $(\nu_4+\nu_5)^0_+ - \nu_4^1$ and $(\nu_4+\nu_5)^0_- - \nu_4^1$ (which had received the same index), the same rotational assignment appeared twice for lines located at different wavenumbers.

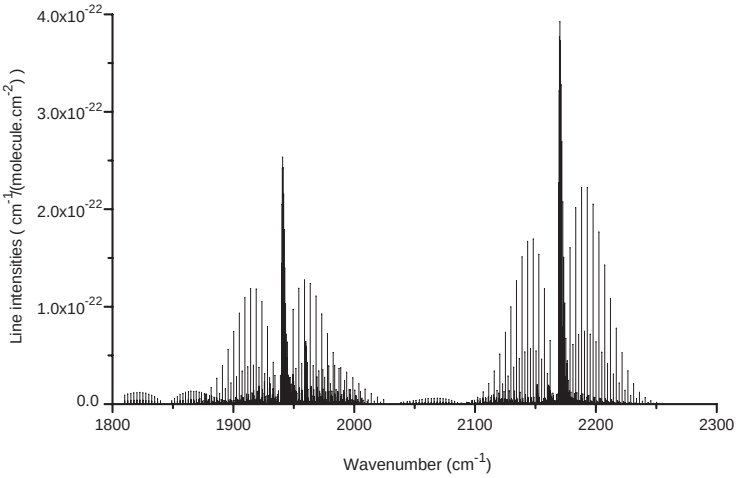

Fig. 2. Synthetic spectrum of the main isotopic species of acetylene between 1800 and 2300 cm^{-1}. This spectrum, computed using the 2000 HITRAN data, shows the $3\nu_5$ spectral region.

2.3.2. *The 7.5-μm spectral region*

In this region (the $2\nu_5$ spectral region between 1248 and 1415 cm^{-1}), data concerning the $(\nu_4+\nu_5)^0_+$ band are present. Data for this band appeared in version 1991 of HITRAN: the line positions originated from the work of Palmer et al. [52] and the line intensities were determined by Podolske et al. [53] from measurements for a limited number of low J R-branch lines. They have been updated in HITRAN 2000 from the work of Vander Auwera [24]. The main difference between the two sets of data is the observation of a significant Herman–Wallis effect in the latter intensities measurements (see Fig. 1 of [24]), interpreted as arising from the combined effects of ℓ-type resonance and Coriolis coupling affecting the upper level of the transition (see [24] for details). The calculated line intensities included in HITRAN 2000 result from the thorough quantitative theoretical treatment performed in [24]. The Herman–Wallis dependence leads to differences in the line intensities between HITRAN 1996 and 2000 ranging from +4.5% for $P(17)$ to −19% for $R(35)$. The line positions and lower level energies were also updated in HITRAN 2000: they were calculated using the model of Kabbadj et al. [54] and constants listed in Table III of that work. The other parameters were left unchanged.

2.3.3. *The 5-μm spectral region*

In this region (the $3\nu_5$ spectral region between 1810 and 2255 cm^{-1}), lines belonging to three cold bands and 15 hot bands have been added. Line positions come mainly from the work of Plíva [39,40], and the line intensities and self-broadening coefficients from the work of Jacquemart et al. [30,31]. Details are given in [31]. As in the 13.6-μm spectral region, line intensities and transition dipole moment squared values were calculated using Herman–Wallis factors. However, because of strong interactions, the $4\nu_5^0$–ν_5^1 band received an empirical treatment: measured line intensities of P- and R-branch lines were adjusted independently of the Q-branch lines, leading to the following vibrational transition dipole moments squared ($1\ D \approx 3.33546 \times 10^{-30}\ C\ m$) and Herman–Wallis

coefficients, defined by Eqs. (1) and (2) of [31]:

P- and R-branch lines: $|R_0|^2 = 2.303 \times 10^{-5}$ D^2, $A_1^{RP} = -2.5 \times 10^{-3}$, $A_2^{RP} = 8.14 \times 10^{-4}$,
Q-branch lines: $|R_0|^2 = 2.125 \times 10^{-5}$ D^2, $A_2^{Q} = -1.24 \times 10^{-3}$.

The self-broadening coefficients have been calculated using an empirical polynomial expansion adjusted to experimental results [39,40] belonging to different bands. Among the experimental data available for air-broadening effects, we have chosen the results of Lambot et al. [55] and Bouanich et al. [56] concerning v_5 lines. The air-broadening coefficients are smoothed values obtained for v_5 lines [55,56]; we have assumed that the air-broadening coefficients have no vibrational dependence, as observed for the self-broadening coefficients. The temperature-dependence exponent, $n = 0.75$, of the air-broadening coefficient is a mean value obtained from Refs. [56–58] that showed that n is noticeably J-dependent, since its experimental values vary from about 0.85 to 0.60 according to J between 1 and 30. Despite this variation, the same rough mean value 0.75 was incorporated for all the lines involved in the 5-μm region, as well as for all other C_2H_2 lines in the database. As far as air-shifting coefficients are concerned, one is only aware of the N_2-shifting coefficients measured by Babay et al. [59] for v_5 lines at room temperature. Although these values are noticeably J-dependent, a rough mean value -0.001 cm^{-1} atm^{-1} has been chosen for all lines.

2.3.4. *The 3-μm spectral region*

In this region (the $5v_5$ spectral region between 3204 and 3359 cm^{-1}), the database contains lines belonging to the two strong cold bands v_3 and $v_2 + (v_4 + v_5)^0_+$. As already stated in Section 1, the original data came from the work of Varanasi et al. [3] and Rinsland et al. [11] for the line positions, Rinsland et al. [11] for the line intensities, Devi et al. [16] for the air-broadening coefficients, and Varanasi et al. [3,17] for the self-broadening coefficients and the temperature dependence of air-broadening coefficients. The line positions and intensities were updated for the 1996 version of the database, from the work of Vander Auwera et al. [23]. These same data are included in HITRAN 2000. The upper levels of both bands interact through a very strong anharmonic resonance, to which ℓ-type resonance in the 010(11) level contributes (see [23] for details). The calculated line positions and intensities included in HITRAN 1996 and 2000 result from the thorough quantitative theoretical treatment performed in [23].

3. Validation of line intensities

Validation of the data chosen to be included in databases is a key problem, since for the users, the knowledge of realistic values of the accuracies is important. The assignments of acetylene lines included in HITRAN are unambiguous, and the accuracy of their wavenumbers is generally satisfactory (absolute uncertainty smaller than 0.001 cm^{-1} for most of the lines, or up to about 0.01 cm^{-1} for some weak lines). Pressure-broadening effects have been (see Section 2.2), or are currently [60], extensively studied, so that reliable expressions exist to model the rotational dependence of air- and self-broadening coefficients. However, their temperature dependence and the air-shifting coefficients are more difficult to obtain. In the literature, published accuracy for line intensities is usually about ±5%, but it can reach ±2% [24]. This accuracy depends on the experimental procedure and on the method used to retrieve line intensities from the spectra. The determination of realistic accuracies is

facilitated by cross comparisons, both between the results obtained by different authors having used different instruments and methods, and between the results obtained from the same experiment but with different methods. In this section, we will recall how line intensities have thus been validated in the 13.6- and 7.5-μm main spectral regions of acetylene. First results concerning the 3-μm region will also be presented.

3.1. The 13.6-μm spectral region

This spectral region being especially important for atmospheric and planetary applications [1–4], the data in the 1996 issue needed to be validated, and possibly improved. New measurements were therefore performed [28,29]. On the whole, line intensities measured in the ν_5 band [28] were found higher than the previous HITRAN 1996 values [32] by about $(14 \pm 7)\%$, whereas they agree with the results of Sun and Varanasi [60] within $(4 \pm 7)\%$. When hot bands are included in the comparison with HITRAN 1996, the results of Refs. [28,29] are on the whole $(11 \pm 3)\%$ higher. The good agreement with the recent results of Ref. [60] seems to show that the intensities of Refs. [28,29] (estimated average accuracy $\pm 5\%$) are probably closer to the true values than HITRAN 1996. They were therefore adopted over the previous ones for the 2000 issue. However, new measurements would be quite useful to remove the doubt.

3.2. The 7.5-μm spectral region

When studying the 5-μm spectral region [30,31], additional spectra were recorded in the 1240–1420 cm^{-1} spectral region, in order to check the purity of the $^{12}C_2H_2$ sample, by comparison with line intensities published by Vander Auwera [24] for the $(\nu_4 + \nu_5)^0_+$ band. A slight systematic discrepancy of $(-1.5 \pm 3.0)\%$ was found between the results of Ref. [30] and those of Ref. [24]. Such a small discrepancy shows that the purity of the sample is satisfactory, so that line intensities deduced in the 5-μm region using the same sample were reliable. Furthermore, this positive cross comparison can be considered as a validation of the HITRAN values in the 7.5-μm region. It is worth noticing that during the study of the 5-μm region, two methods of determination of line parameters from experimental spectra, built independently by different teams, were compared successfully and then validated [30,61,62].

3.3. The 3-μm spectral region

3.3.1. Interest of this spectral region

In this spectral region, the two strong ν_3 and $\nu_2 + (\nu_4 + \nu_5)^0_+$ cold bands occur, as well as numerous hot bands. They are observable in the circumstellar shell of cool carbon stars such as IRC + 10216 [11,12], so that their assignment was achieved as early as 1982 by Rinsland et al. [11], who also measured line intensities, mainly in the cold bands. Line intensities were measured again by Vander Auwera et al. [23] in the cold bands, but the hot bands are still poorly known. That is why an exhaustive study of these bands was initiated at LPMA (Paris) using FT spectra recorded at GSMA (Reims). The very first step of this work will be presented in the following: it concerns a cross comparison between ν_3 and $\nu_2 + (\nu_4 + \nu_5)^0_+$ line intensities obtained with the GSMA spectra, and those previously published [23] and currently present in the 2000 HITRAN edition [41].

Table 2
Experimental conditions and characteristics of the spectra recorded in the 3-μm region in Reims

Commercial sample (*Air Liquide Alphagaz*)	
Natural C_2H_2	97.760% of $^{12}C_2H_2$
Stated purity	99.55%
Additional cell containing OCS	
Absorbing path	31 cm
Pressure	0.5 Torr[a]
Temperature	≈ 296.5 K
Maximum path difference	140.5 cm
Unapodized FWHM resolution	3.56×10^{-3} cm^{-1}
SNR	≈ 100
Collimator focal length	1040 mm
Nominal iris radius	2.25 mm
Free spectral range	1975–3950 cm^{-1}

Spectrum #	Effective iris radius (mm)[b]	Total pressure ±0.5%[c] (Torr)[a]	Absorbing path ±0.01 cm[c]	Temperature ±0.5 K[c]
1	2.36(2)	0.404	3.624	296.75
2	2.30(2)	0.424	3.624	296.85
3	2.37(2)	0.707	3.624	296.75
4	2.37(2)	0.708	3.624	296.85
5	2.32(2)	0.990	3.624	296.55
6	2.37(2)	2.917	3.624	296.85
7	2.36(2)	2.920	3.624	296.75
8	2.36(2)	6.989	3.624	296.85
9	2.37(3)	6.920	3.624	296.95
10	2.32(4)	10.451	3.624	296.45

[a] 1 Torr = 1.333 hPa.
[b] 1 SD between parentheses in unit of the last digit.
[c] Absolute uncertainty.

3.3.2. Experimental details and methodology

Experimental conditions and characteristics of the spectra obtained with the GSMA step-by-step interferometer [63,64] have been gathered in Table 2. This apparatus was used with a globar as radiation source, CaF_2 splitting and mixing plates, InSb detector, and CaF_2 cell windows. The total recording time of an interferogram is about 4 h, with a total integration time of 10 ms per point. The analysis procedure is the same as in Ref. [30], so that only specific considerations will be mentioned here.

A small amount of OCS was put in a second cell crossed by the beam (see Table 2). OCS lines are then observable around 3.4 μm. About 20 of these lines, between 2910 and 2930 cm^{-1}, have been used to calibrate the wavenumber scale of the spectra, and to determine the effective iris radius needed to model the apparatus function. For the calibration of the wavenumber scale, we used line positions of HITRAN [32]. The fact that the OCS lines are very narrow compared with the apparatus

function, allowed one to deduce very significant average values of the effective iris radius in each spectrum. One observed that almost the same value was obtained for all the spectra (see Table 2), a value slightly larger than the nominal value, as expected.

The knowledge of the phase error is necessary to avoid errors in the determination of line parameters, mainly the transition wavenumbers. The average phase error determined around 2920 cm^{-1} (about +0.06 rad) from OCS lines, was found different from that measured around 3300 cm^{-1} (about −0.07 rad) from C_2H_2 lines. Inside the domain of C_2H_2 lines, and for each spectrum, a linear wavenumber dependence of the phase error was adjusted to the obtained values. These linear dependences of the phase error were further used in the line fits. Indeed, despite the small values of the phase error, neglecting it would have led to errors in C_2H_2 line positions up to 0.0003 cm^{-1}, and neglecting the wavenumber dependence of this phase error would have led to errors up to 0.00015 cm^{-1}.

The wavenumber calibration was very precise (relative uncertainty smaller than 0.00005 cm^{-1}). Taking into account the accuracy announced in HITRAN for the OCS wavenumbers (namely between 0.001 and 0.0001 cm^{-1}), absolute $^{12}C_2H_2$ line positions have been obtained with an average accuracy better than 0.001 cm^{-1}.

To deduce line parameters, a multispectrum fitting method was used [62]. The details on this procedure have already been given in a previous paper [30]. A Voigt profile was used to calculate the absorption coefficient, the collisional narrowing being considered as negligible under our experimental conditions. Because of the relatively low pressures, it was advisable to fix the self-broadening coefficients during the line fits. For that, we used the values introduced in HITRAN in the 5-μm spectral region (see Section 2.3.3). To model the rotational dependence of the self-broadening coefficients, we tried the more elaborate expression proposed by El Hachtouki and Vander Auwera [47], but the consequences on retrieved line parameters appeared negligible (average difference about 0.1%), in our pressure conditions and for the set of studied lines. Self-shifting coefficients were let free and could be determined; however, the obtained preliminary values are not given in this paper, because we plan to improve them when more spectra, recorded at Paris from another interferometer, will have been treated together with the spectra recorded at Reims.

To be able to compare directly our line intensities with those present in HITRAN [41], in the determination of line intensities we used the partition function calculated by Gamache et al. in 1990 [65], instead of the one published in 2000 [66], because the HITRAN data are issued from Ref. [23] in which the partition function of Ref. [65] was used. Note that the values of the two partition functions, at the standard temperature of 296 K, differ by 1.6%, so that transition dipole moment squared values, deduced using these partition functions, would also differ by the same amount; however, the consequences on line intensities would be totally negligible in the present case, since they come from spectra recorded with temperatures close to 296 K.

3.3.3. Results

About 110 line positions and intensities have been measured in the ν_3 and $\nu_2 + (\nu_4 + \nu_5)^0_+$ bands. These results have been assembled in Table 3. The statistical uncertainty of line positions is 0.00005 cm^{-1} on the average. That is why five decimal digits have been given in Table 3, although the absolute uncertainty is between 0.0001 and 0.001 cm^{-1} (see Section 3.3.2). On the whole, a good agreement is found between the line positions measured in this work and those present in

Table 3
Comparisons between line positions and intensities of HITRAN 2000 [41] (issued from Ref. [23]) and experimental line positions and intensities obtained in this work, for the ν_3 and $\nu_2+(\nu_4+\nu_5)^0_+$ cold bands of $^{12}C_2H_2$[a]

Line	Position obs (this work)	Position HITRAN	obs-HITRAN 10^{-3} cm^{-1}	Intensity obs (this work)	Intensity HITRAN	(obs-HITRAN)/obs %
ν_3						
Pee33	3211.60187	3211.601651	0.22	2.00E − 21	1.935E − 21	3.25
Pee32	3214.34222	3214.342372	−0.15	9.36E − 22	9.137E − 22	2.38
Pee31	3217.06632	3217.066339	−0.02	3.88E − 21	3.838E − 21	1.08
Pee30	3219.77449	3219.774514	−0.02	1.78E − 21	1.771E − 21	0.51
Pee29	3222.46734	3222.467204	0.14	7.46E − 21	7.262E − 21	2.65
Pee28	3225.14405	3225.143978	0.07	3.38E − 21	3.271E − 21	3.22
Pee27	3227.80515	3227.805295	−0.14	1.33E − 20	1.310E − 20	1.50
Pee26	3230.45077	3230.450800	−0.03	5.83E − 21	5.757E − 21	1.25
Pee25	3233.08093	3233.080988	−0.06	2.26E − 20	2.249E − 20	0.49
Pee24	3235.69614	3235.696132	0.01	9.77E − 21	9.638E − 21	1.35
Pee23	3238.29645	3238.296322	0.13	3.74E − 20	3.669E − 20	1.90
Pee22	3240.88208	3240.882075	0.00	1.56E − 20	1.531E − 20	1.86
Pee21	3243.45358	3243.453563	0.02	5.68E − 20	5.677E − 20	0.05
Pee20	3246.01127	3246.011304	−0.03	2.31E − 20	2.306E − 20	0.17
Pee19	3248.55572	3248.555562	0.16	8.48E − 20	8.313E − 20	1.97
Pee18	3251.08683	3251.086863	−0.03	3.28E − 20	3.282E − 20	−0.06
Pee17	3253.60558	3253.605405	0.18	1.16E − 19	1.149E − 19	0.95
Pee16	3256.11201	3256.112113	−0.10	4.39E − 20	4.403E − 20	−0.30
Pee15	3258.60688	3258.606936	−0.06	1.52E − 19	1.494E − 19	1.71
Pee14	3261.09038	3261.090405	−0.02	5.55E − 20	5.545E − 20	0.09
Pee13	3263.56288	3263.562906	−0.03	1.84E − 19	1.821E − 19	1.03
Pee12	3266.02490	3266.024783	0.12	6.50E − 20	6.526E − 20	−0.40
Pee11	3268.47663	3268.476542	0.09	2.08E − 19	2.065E − 19	0.72
Pee10	3270.91847	3270.918449	0.02	7.17E − 20	7.119E − 20	0.71
Pee 9	3273.35075	3273.350709	0.04	2.14E − 19	2.160E − 19	−0.93
Pee 8	3275.77359	3275.773520	0.07	7.02E − 20	7.108E − 20	−1.25
Pee 7	3278.18739	3278.187365	0.02	2.05E − 19	2.048E − 19	0.10
Pee 6	3280.59213	3280.592196	−0.07	6.30E − 20	6.343E − 20	−0.68
Pee 3	3287.75426	3287.754368	−0.11	1.13E − 19	1.129E − 19	0.09
Pee 2	3290.12459	3290.124900	−0.31	2.61E − 20	2.593E − 20	0.65
Ree 1	3299.52058	3299.520505	0.07	7.76E − 20	7.874E − 20	−1.47
Ree 3	3304.16654	3304.166729	−0.19	1.46E − 19	1.474E − 19	−0.96
Ree 4	3306.47609	3306.476223	−0.13	5.81E − 20	5.839E − 20	−0.50
Ree 5	3308.77647	3308.776525	−0.06	1.94E − 19	1.974E − 19	−1.75
Ree 6	3311.06734	3311.067487	−0.15	6.98E − 20	7.124E − 20	−2.06
Ree 7	3313.34852	3313.348542	−0.02	2.18E − 19	2.239E − 19	−2.71
Ree 8	3315.61974	3315.619792	−0.05	7.43E − 20	7.608E − 20	−2.40
Ree 9	3317.88055	3317.880408	0.14	2.24E − 19	2.270E − 19	−1.34
Ree10	3320.13066	3320.130748	−0.09	7.30E − 20	7.364E − 20	−0.88
Ree11	3322.36962	3322.369710	−0.09	2.14E − 19	2.107E − 19	1.54
Ree13	3326.81243	3326.812475	−0.05	1.79E − 19	1.813E − 19	−1.28
Ree14	3329.01553	3329.015606	−0.08	5.46E − 20	5.461E − 20	−0.02
Ree15	3331.20548	3331.205620	−0.14	1.45E − 19	1.457E − 19	−0.48

Table 3 (*continued*)

Line	Position obs (this work)	Position HITRAN	obs-HITRAN 10^{-3} cm^{-1}	Intensity obs (this work)	Intensity HITRAN	(obs-HITRAN)/obs %
Ree17	3335.54469	3335.545011	−0.32	1.09E − 19	1.100E − 19	−0.92
Ree18	3337.69301	3337.693082	−0.07	3.15E − 20	3.116E − 20	1.08
Ree20	3341.94426	3341.944206	0.05	2.20E − 20	2.155E − 20	2.05
Ree21	3344.04597	3344.045803	0.17	5.20E − 20	5.268E − 20	−1.31
Ree22	3346.13173	3346.131748	−0.02	1.43E − 20	1.412E − 20	1.26
Ree23	3348.20058	3348.200852	−0.27	3.41E − 20	3.359E − 20	1.50
Ree24	3350.25280	3350.252893	−0.09	9.05E − 21	8.769E − 21	3.10
Ree25	3352.28734	3352.287448	−0.11	2.08E − 20	2.035E − 20	2.16
Ree27	3356.30355	3356.303646	−0.10	1.20E − 20	1.172E − 20	2.33
Ree28	3358.28542	3358.285091	0.33	2.98E − 21	2.912E − 21	2.28
$v_2 + (v_4 + v_5)^0_+$						
Pee30	3207.37933	3207.379655	−0.32	2.61E − 21	2.524E − 21	3.30
Pee29	3210.01650	3210.016305	0.20	1.05E − 20	1.025E − 20	2.38
Pee28	3212.64085	3212.640735	0.11	4.70E − 21	4.562E − 21	2.94
Pee27	3215.25319	3215.253045	0.14	1.82E − 20	1.804E − 20	0.88
Pee26	3217.85355	3217.853528	0.02	8.09E − 21	7.830E − 21	3.21
Pee25	3220.44225	3220.442178	0.07	3.07E − 20	3.018E − 20	1.69
Pee24	3223.01937	3223.019323	0.05	1.32E − 20	1.275E − 20	3.41
Pee23	3225.58516	3225.585108	0.05	4.76E − 20	4.784E − 20	−0.50
Pee22	3228.13981	3228.139683	0.13	1.98E − 20	1.968E − 20	0.61
Pee21	3230.68338	3230.683053	0.33	7.17E − 20	7.187E − 20	−0.24
Pee19	3235.73859	3235.738359	0.23	1.00E − 19	1.022E − 19	−2.20
Pee16	3243.24423	3243.244096	0.13	5.15E − 20	5.188E − 20	−0.74
Pee15	3245.72635	3245.726226	0.12	1.75E − 19	1.738E − 19	0.69
Pee13	3250.66235	3250.662417	−0.07	2.09E − 19	2.066E − 19	1.15
Pee12	3253.11640	3253.116395	0.00	7.32E − 20	7.321E − 20	−0.01
Pee11	3255.56149	3255.561522	−0.03	2.33E − 19	2.293E − 19	1.59
Pee10	3257.99777	3257.997561	0.21	7.82E − 20	7.826E − 20	−0.08
Pee 9	3260.42538	3260.425454	−0.07	2.40E − 19	2.354E − 19	1.92
Pee 8	3262.84448	3262.844474	0.01	7.73E − 20	7.683E − 20	0.61
Pee 7	3265.25511	3265.255045	0.07	2.17E − 19	2.197E − 19	−1.24
Pee 6	3267.65737	3267.657264	0.11	6.76E − 20	6.766E − 20	−0.09
Pee 5	3270.05137	3270.051374	0.00	1.78E − 19	1.802E − 19	−1.24
Pee 4	3272.43720	3272.437274	−0.07	5.13E − 20	5.069E − 20	1.19
Pee 3	3274.81489	3274.814823	0.07	1.18E − 19	1.189E − 19	−0.76
Pee 2	3277.18445	3277.184485	−0.04	2.76E − 20	2.725E − 20	1.27
Pee 1	3279.54582	3279.545903	−0.08	4.22E − 20	4.170E − 20	1.18
Ree 0	3284.24405	3284.244315	−0.27	1.43E − 20	1.400E − 20	2.10
Ree 1	3286.58112	3286.581063	0.06	8.39E − 20	8.295E − 20	1.13
Ree 2	3288.90964	3288.909686	−0.05	4.17E − 20	4.050E − 20	2.88
Ree 3	3291.22975	3291.229789	−0.04	1.55E − 19	1.565E − 19	−0.97
Ree 4	3293.54128	3293.541372	−0.09	6.10E − 20	6.227E − 20	−2.08
Ree 5	3295.84413	3295.843996	0.13	2.06E − 19	2.118E − 19	−2.82
Ree 6	3298.13821	3298.138308	−0.10	7.61E − 20	7.699E − 20	−1.17

Table 3 (*continued*)

Line	Position obs (this work)	Position HITRAN	obs-HITRAN 10^{-3} cm^{-1}	Intensity obs (this work)	Intensity HITRAN	(obs-HITRAN)/obs %
Ree 7	3300.42323	3300.423247	−0.02	2.46E − 19	2.440E − 19	0.81
Ree 8	3302.69903	3302.699157	−0.13	8.29E − 20	8.363E − 20	−0.88
Ree 9	3304.96538	3304.965472	−0.09	2.45E − 19	2.520E − 19	−2.86
Ree10	3307.22208	3307.222116	−0.04	8.41E − 20	8.262E − 20	1.76
Ree11	3309.46896	3309.468790	0.17	2.36E − 19	2.391E − 19	−1.31
Ree12	3311.70567	3311.705602	0.07	7.50E − 20	7.548E − 20	−0.64
Ree13	3313.93193	3313.931949	−0.02	2.14E − 19	2.108E − 19	1.50
Ree14	3316.14751	3316.147670	−0.16	6.46E − 20	6.436E − 20	0.37
Ree15	3318.35222	3318.352355	−0.13	1.75E − 19	1.741E − 19	0.51
Ree16	3320.54568	3320.545818	−0.14	5.16E − 20	5.152E − 20	0.16
Ree17	3322.72765	3322.727775	−0.13	1.33E − 19	1.352E − 19	−1.65
Ree18	3324.89779	3324.897975	−0.18	3.86E − 20	3.887E − 20	−0.70
Ree19	3327.05591	3327.056086	−0.18	9.90E − 20	9.912E − 20	−0.12
Ree20	3329.20158	3329.201813	−0.23	2.80E − 20	2.770E − 20	1.07
Ree21	3331.33478	3331.334926	−0.15	6.92E − 20	6.869E − 20	0.74
Ree22	3333.45483	3333.455087	−0.26	1.89E − 20	1.868E − 20	1.16
Ree23	3335.56186	3335.562197	−0.34	4.56E − 20	4.507E − 20	1.16
Ree24	3337.65549	3337.655694	−0.20	1.23E − 20	1.193E − 20	3.01
Ree27	3343.85262	3343.852750	−0.13	1.64E − 20	1.654E − 20	−0.85
Ree28	3345.88967	3345.889965	−0.29	4.30E − 21	4.153E − 21	3.42
Ree29	3347.91217	3347.912330	−0.16	9.43E − 21	9.262E − 21	1.78
Ree30	3349.91960	3349.919816	−0.22	2.35E − 21	2.266E − 21	3.57
Ree31	3351.91197	3351.912181	−0.21	5.09E − 21	4.925E − 21	3.24

[a]Line positions are in cm^{-1}, and line intensities in cm^{-1}/(molecule cm^{-2}) at 296 K for pure $^{12}C_2H_2$. The "ee" mentioned in the line assignments means that the upper and lower rotational levels of the involved transitions have both the *e* symmetry type.

HITRAN [41] (see Fig. 3), since the average difference between our wavenumbers and those of HITRAN is $(-0.02 \pm 0.13) \times 10^{-3}$ cm^{-1} for the ν_3 band, and $(-0.04 \pm 0.15) \times 10^{-3}$ cm^{-1} for the $\nu_2 + (\nu_4 + \nu_5)^0_+$ band. Note that Fig. 3 does not exhibit striking discrepancies between the database line positions and ours, except for the $\nu_2 + (\nu_4 + \nu_5)^0_+$ band, where a slight linear distortion can be detected, but on the mean not exceeding ± 0.0002 cm^{-1}, in accordance with the accuracies stated in this work and in Refs. [23,41].

Intensities measured in this work have an average statistical uncertainty of 0.5%, and a mean accuracy of ±5%. They can be directly compared with HITRAN line intensities [41], preliminarily converted to pure $^{12}C_2H_2$. The results of these comparisons are given in Table 3 and illustrated in Fig. 4, showing that the agreement is on the whole very satisfactory: the average of the discrepancy between our line intensities and those of HITRAN is (0.5 ± 1.5)% for the ν_3 band, and (0.6 ± 1.7)% for the $\nu_2 + (\nu_4 + \nu_5)^0_+$ band. Furthermore, no large discrepancy is observed since the maximum difference between the database line intensities and our experimental values is about 3.5%, a value compatible with the accuracies stated in this work and in Refs. [23,41]. However, one should note

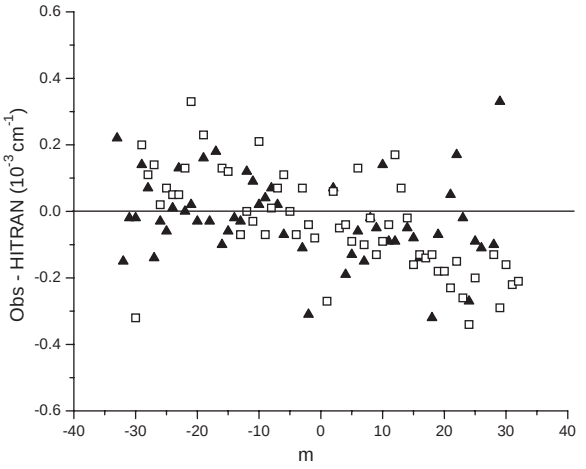

Fig. 3. Comparison between HITRAN line positions [41] and experimental line positions obtained in this work. Solid triangles are for the ν_3 band, and open squares are for the $\nu_2+(\nu_4+\nu_5)^0_+$ band. m is the running index equal to $-J''$ in the P branch and $J''+1$ in the R branch.

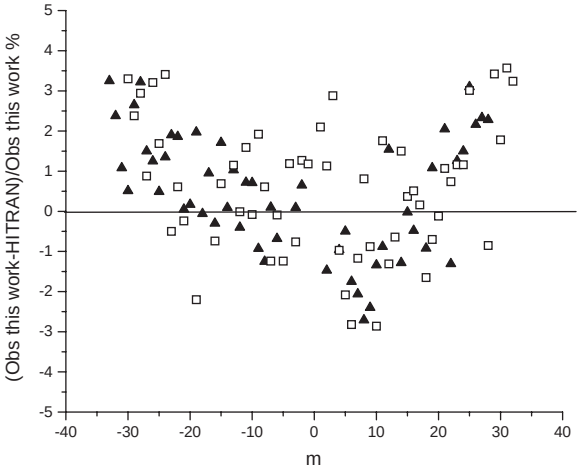

Fig. 4. Comparison between HITRAN line intensities [41] and experimental line intensities obtained in this work. Solid triangles are for the ν_3 band, and open squares are for the $\nu_2+(\nu_4+\nu_5)^0_+$ band. m is the running index equal to $-J''$ in the P branch and $J''+1$ in the R branch.

that the two series of data seem to slightly diverge from one another for high J values, which correspond to weak lines in the studied spectra.

4. Conclusion and recommendations

The main recent improvements of HITRAN for C_2H_2 have concerned the 13.6- and 7.5-μm spectral regions (improved line intensities) [24,28,29], and the 5-μm region (previously absent) [30,31].

To improve the C_2H_2 data in HITRAN, we will make some suggestions that have been partly taken into account in the 2000 edition including the updates of 2001.

- For the main isotopomer, new results should be introduced in spectral regions useful for some applications (atmospheric, planetary, or astrophysical studies, but also wavenumber calibrations), and that are presently absent or incomplete in HITRAN. It is worth noting that hot bands should not be omitted, since their total absorption is on the whole non-negligible. Furthermore, their knowledge allows one to improve global theoretical calculations, leading to a computation of more accurate and coherent linelists in the entire spectrum [33]. For example, the $5\nu_5$ spectral region at 3 μm could be completed, since numerous hot bands are presently missing. In the same way, the $10\nu_5$ spectral region at 1.5 μm studied by El Hachtouki and Vander Auwera [47] should be advantageously added in HITRAN, as well as the absolute line wavenumbers of Ref. [43] between 7060 and 9880 cm^{-1}. In the 13.6-μm region, the two-quantum hot bands studied by Weber et al. [67] have also a theoretical interest, but however, no line intensity data are available for these bands.

- As for the hot bands of the main isotopomer, lines of the $^{12}C^{13}CH_2$ isotopic species have a non-negligible absorption. Let us recall that at the present time, data concerning this isotopomer are present in HITRAN only for two bands (see Table 1). Thus, available experimental data should be compiled and introduced in HITRAN. For example, recent results at 3 [44] and 1.5 μm [47] could be taken into account.
- The quality of the synthetic line lists (positions and intensities) could be improved by using a global model [33]. This concerns first the region where HITRAN line positions and line intensities have been calculated using a theoretical model that takes into account the interactions only through empirical expressions, namely the 5-μm region.
- The notation of Plíva seems well suited to label levels. It will be adopted and fully given in the next edition of HITRAN. For the rotational assignment of lines, we suggest adding systematically the character *e* or *f*, even when there is no ambiguity.
- The air-broadening coefficients and their temperature dependence should be improved, taking into account new experimental results of Sun and Varanasi [60], concerning the measurements of nitrogen-broadening coefficients in the 13.6-μm spectral region, together with their temperature dependence. These values could be extrapolated for all bands assuming that there is no vibrational dependence.
- The self-broadening coefficients could be slightly improved, compiling new experimental results, and using a more precise empirical expansion than in Ref. [31], similar to the one used by El Hachtouki and Vander Auwera [47] or Sinclair et al. [68], and which could be extrapolated for all bands assuming that there is no vibrational dependence.
- The air- and self-broadening coefficients presently in the database should at least be homogenized (at the present time, these data have different origins according to the spectral region).
- As far as air-pressure-shifting coefficients are concerned, the experimental N_2-shifting coefficients of Babay et al. [59] could be introduced in the database for the ν_5 band. As pressure shifts can have a vibrational dependence, the mean value -0.001 cm^{-1}atm^{-1}, put for all lines in the 5-μm spectral region, can also be used for other bands or in other regions, in the absence of experimental data, but one has to bear in mind that this is only a rough estimation.

To conclude, one should point out the fact that users need to know not only the precision in relative values of line parameters, but also their accuracy. The error codes mentioned for acetylene in HITRAN, which should indicate realistic accuracies, were homogenized in the updates of 2001. They are summarized in Table 4. On the whole, absolute line positions are known to be better than 0.001 cm^{-1} (error code 4), except in the 5-μm spectral region (error code 3). Line intensities have received the error code 6 (absolute error range between 2% and 5%), except in the 7.5-μm region (error code 7: absolute error range between 1% and 2%), and for lines belonging to some weak bands of the 5-μm region (error code 5 or 4). As the expressions used to generate air-broadening coefficients appeared very reliable in the involved spectral regions, for which no vibrational dependence was found, the error code 6 (2–5%) should match the experimental accuracy of measurement and be quoted for all lines. In the next issue, individual error codes will be reported for the other line parameters. Taking into account the quality of the present data, we suggest an error code 6 for all self-broadening coefficients. The exponent *n* of the temperature dependence of air-broadening coefficients is, at the present time, not well known, so that an error code 4 (10–20%) should be quoted for all lines. Because of the poor knowledge of air-shifting coefficients, an error code 4 (10–20%)

Table 4
Summary of error codes for acetylene in the HITRAN update of 2001[a]

Spectral region (μm)	Line positions	Line intensities[b]	Air-broadening coefficients	Self-broadening coefficients	Temperature dependence of air broadening	Air-shifting coefficients
13.6	4	6	4 or 5 (6)	(6)	(4)	(4 or 3)
7.5	4	7	6	(6)	(4)	(3)
5	3	6, 5, or 4	6	(6)	(4)	(3)
3	4	6	6	(6)	(4)	(3)

Convention for error codes in HITRAN
For line positions
3: $\geqslant 0.001$ and < 0.01 cm^{-1}.
4: $\geqslant 0.0001$ and < 0.001 cm^{-1}.

For other line parameters
3: $\geqslant 20\%$.
4: $\geqslant 10\%$ and $< 20\%$.
5: $\geqslant 5\%$ and $< 10\%$.
6: $\geqslant 2\%$ and $< 5\%$.
7: $\geqslant 1\%$ and $< 2\%$.

[a]Between parentheses are error codes to adopt in the next issue for the current line parameters. Others are those present in the 2001 update.

[b]Reported error codes are for $^{12}C_2H_2$. For $^{12}C^{13}CH_2$, all line parameters have the same error codes than $^{12}C_2H_2$, except for line intensities (code 4).

should be reported for ν_5 lines, and a realistic code 3 (absolute uncertainty larger than 20%) could be chosen for all other lines. For the $^{12}C^{13}CH_2$ molecule, the same error codes have been, or could be, adopted, except for all line intensities which have received the code 4 (10–20%).

Acknowledgements

The authors acknowledge J.-J. Plateaux, X. Thomas, P. Von der Heyden, and D. Décatoire from GSMA (Reims), as well as A. Valentin from LPMA (Paris), for their contribution in some parts of this work. JVDA acknowledges financial support from the Fonds National de la Recherche Scientifique (FNRS, Belgium).

References

[1] Ridgway ST. Jupiter: identification of ethane and acetylene. Astrophys J 1974;187:L41–3.
[2] Combes M, Encrenaz T, Vapillon L, Zéau Y, Lesqueren C. Confirmation of the identification of C_2H_2 and C_2H_6 in the Jovian atmosphere. Astron Astrophys 1974;34:33–5.
[3] Varanasi P, Giver LP, Valero FPJ. Infrared absorption by acetylene in the 12–14 μm region at low temperatures. JQSRT 1983;30:497–504.
[4] Varanasi P. Intensity and linewidth measurements in the 13.7-μm fundamental bands of $^{12}C_2H_2$ and $^{12}C^{13}CH_2$ at planetary atmospheric temperatures. JQSRT 1992;47:263–74.

[5] Encrenaz Th, Feuchtgruber H, Atreya SK, Bézard B, Lellouch E, Bishop J, Edgington S, de Graauw Th, Griffin M, Kessler MF. ISO observations of Uranus: the stratospheric distribution of C_2H_2 and the eddy diffusion coefficient. Astron Astrophys 1998;333:L43–6.
[6] Whitby RA, Altwhicker ER. Acetylene in the atmosphere: sources, representative ambient concentrations and ratios to other hydrocarbons. Atmos Environ 1978;12:1289–96.
[7] Kanakidou M, Bonsang B, Le Roulley JC, Lambert G, Martin D, Sennequier G. Marine source of atmospheric acetylene. Nature 1988;333:51–2.
[8] Harley RA, Cass GR. Modeling the atmospheric concentrations of individual volatile organic compounds. Atmos Environ 1995;29:905–22.
[9] Mohan Rao AM, Pandit GG, Sain P, Sharma S, Krishnamoorthy TM, Nambi KSV. Non-methane hydrocarbons in industrial locations of Bombay. Atmos Environ 1997;31:1077–85.
[10] Goldman A, Murcray FJ, Blatherwick RD, Gillis JR, Bonomo FS, Murcray FH, Murcray DG. Identification of acetylene C_2H_2 in infrared atmospheric absorption spectra. J Geophys Res 1981;86:12143–6.
[11] Rinsland CP, Baldacci A, Rao KN. Acetylene bands observed in carbon stars: a laboratory study and an illustrative example of its application to IRC + 10216. Astrophys J Suppl Ser 1982;49:487–513.
[12] Hillman JJ, Jennings DE, Halsey GW, Nadler S, Blass WE. An infrared study of the bending region of acetylene. J Mol Spectrosc 1991;146:389–401.
[13] Cernicharo J, Yamamura I, González-Alfonso E, De Jong T, Heras A, Escribano R, Ortigoso J. The ISO/SWS spectrum of IRC + 10216: the vibrational bands of C_2H_2 and HCN. Astrophys J 1999;526:L41–4.
[14] Aoki W, Tsuji T, Ohnaka K. Infrared spectra of carbon stars observed by the ISO SWS. II. HCN and C_2H_2 bands at 14 μm. Astron Astrophys 1999;350:945–54.
[15] Rothman LS, Gamache RR, Goldman A, Brown LR, Toth RA, Pickett HM, Poynter RL, Flaud JM, Camy-Peyret C, Barbe A, Husson N, Rinsland CP, Smith MAH. The HITRAN database: 1986 edition. Appl Opt 1987;26:4058–97.
[16] Devi VM, Benner DC, Rinsland CP, Smith MAH, Sidney BD. Tunable diode laser measurements of N_2- and air-broadened halfwidths: lines in the $(v_4 + v_5)^0$ band of $^{12}C_2H_2$ near 7.4 μm. J Mol Spectrosc 1985;114:49–53.
[17] Varanasi P, Giver LP, Valero FPJ. Measurements of nitrogen-broadened line widths of acetylene at low temperatures. JQSRT 1983;30:505–9.
[18] Herman M, Liévin J, Vander Auwera J, Campargue A. Global and accurate vibration Hamiltonians from high-resolution molecular spectroscopy. In: Prigogine I, Rice SA, editors. Advances in chemical physics, vol. 108. New York: Wiley, 1999.
[19] Zhilinskii BI, El Idrissi MI, Herman M. The vibrational energy pattern in acetylene (VI): inter- and intra-polyad structures. J Chem Phys 2000;113:7885–90.
[20] Weber M, Blass WE, Salanave JL. Tunable diode-laser measurements of the 14 μm line strengths in C_2H_2. JQSRT 1989;42:437–43.
[21] Weber M, Blass WE, Halsey GW, Hillman JJ, Maguire WC. ℓ-Resonance effects in the v_5, $2v_5 - v_5$, and $v_4 + v_5 - v_4$ bands of C_2H_2 and $^{13}C^{12}CH_2$ near 13.7 μm. Spectrochim Acta 1992;48A:1203–26.
[22] Weber M, Blass WE, Halsey GW, Hillman JJ. ℓ-Resonance perturbation of IR intensities in $^{12}C_2H_2$ near 13.7 μm. J Mol Spectrosc 1994;165:107–23.
[23] Vander Auwera J, Hurtmans D, Carleer M, Herman M. The v_3 fundamental in C_2H_2. J Mol Spectrosc 1993;157: 337–57.
[24] Vander Auwera J. Absolute intensities measurements in the $v_4 + v_5$ band of $^{12}C_2H_2$: analysis of Herman–Wallis effects and forbidden transitions. J Mol Spectrosc 2000;201:143–50.
[25] Perevalov VI, Lobodenko EI, Teffo JL. Reduced effective hamiltonian for global fitting of C_2H_2 rovibrational lines. In: Proceedings of the XIIth Symposium and School on High-Resolution Molecular Spectroscopy, St. Petersburg, Russia. SPIE 1997;3090:143–9.
[26] Lyulin OM, Perevalov VI, Tashkun SA, Teffo JL. Global fitting of the vibrational–rotational line positions of acetylene molecule. In: Proceedings of the XIIIth Symposium and School on High-Resolution Molecular Spectroscopy, Tomsk, Russia. SPIE 2000;4063:126–33.
[27] Teffo JL, Lyulin OM, Perevalov VI, Lobodenko EI. Application of the effective operator approach to the calculation of $^{12}C^{16}O_2$ line intensities. J Mol Spectrosc 1998;187:28–41.
[28] Mandin JY, Dana V, Claveau C. Line intensities in the v_5 band of acetylene $^{12}C_2H_2$. JQSRT 2000;67:429–46.

[29] Jacquemart D, Claveau C, Mandin JY, Dana V. Line intensities of hot bands in the 13.6-μm spectral region of acetylene $^{12}C_2H_2$. JQSRT 2001;69:81–101.
[30] Jacquemart D, Mandin JY, Dana V, Régalia-Jarlot L, Thomas X, Von der Heyden P. Multispectrum fitting measurements of line parameters for 5-μm cold bands of acetylene. JQSRT 2002;75:397–422.
[31] Jacquemart D, Mandin JY, Dana V, Régalia-Jarlot L, Plateaux JJ, Décatoire D, Rothman LS. The spectrum of acetylene 5-μm region from new line parameter measurements. JQSRT 2003;76:237–67.
[32] Rothman LS, Rinsland CP, Goldman A, Massie ST, Edwards DP, Flaud JM, Perrin A, Camy-Peyret C, Dana V, Mandin JY, Schœder J, McCann A, Gamache RR, Wattson RB, Yoshino K, Chance KV, Jucks KW, Brown LR, Nemtchinov V, Varanasi P. The HITRAN molecular spectroscopic database and HAWKS (HITRAN Atmospheric Workstation): 1996 edition. JQSRT 1998;60:665–710.
[33] Perevalov VI, Lyulin OM, Jacquemart D, Claveau C, Teffo JL, Dana V, Mandin JY, Valentin A. Global fitting of line intensities of acetylene molecule in the infrared using the effective operator approach. J Mol Spectrosc 2003;218:180–9.
[34] Abbouti Temsamani M, Herman M. The vibrational energy levels in acetylene $^{12}C_2H_2$: towards a regular pattern at higher energies. J Chem Phys 1995;102:6371–84.
[35] Abbouti Temsamani M, Herman M. The vibrational energy pattern in $^{12}C_2H_2$ (II): vibrational clustering and rotational structure. J Chem Phys 1996;105:1355–62.
[36] El Idrissi MI, Liévin J, Campargue A, Herman M. The vibrational energy pattern in acetylene (IV): updated global vibration constants for $^{12}C_2H_2$. J Chem Phys 1999;110:2074–86.
[37] Kellman ME. Approximate constants of motion for vibrational spectra of many-oscillator systems with multiple anharmonic resonances. J Chem Phys 1990;93:6630–5.
[38] Kellman ME, Chen G. Approximate constants of motion and energy transfer pathways in highly excited acetylene. J Chem Phys 1991;95:8671–2.
[39] Plíva J. Spectrum of acetylene in the 5-micron region. J Mol Spectrosc 1972;44:145–64.
[40] Plíva J. Molecular constants for the bending modes of acetylene $^{12}C_2H_2$. J Mol Spectrosc 1972;44:165–82.
[41] Rothman LS, Barbe A, Benner DC, Brown LR, Camy-Peyret C, Carleer MR, Chance KV, Clerbaux C, Dana V, Devi VM, Fayt A, Flaud JM, Gamache RR, Goldman A, Jacquemart D, Jucks KW, Lafferty WJ, Mandin JY, Massie ST, Nemtchinov V, Newnham D, Perrin A, Rinsland CP, Schrœder J, Smith K, Smith MAH, Tang K, Toth RA, Vander Auwera J, Varanasi P, Yoshino K. The HITRAN molecular spectroscopic database: edition of 2000 including updates through 2001. JQSRT, doi:10.1016/S0022-4073(03)00146-8.
[42] Herman M, Campargue A, El Idrissi MI, Vander Auwera J. Vibrational spectroscopic database on acetylene $X^1\Sigma_g^+$ ($^{12}C_2H_2$, $^{12}C_2D_2$ and $^{13}C_2H_2$). J Phys Chem Ref Data, in press.
[43] Vander Auwera J, El Hachtouki R, Brown LR. Absolute line wavenumbers in the near infrared: $^{12}C_2H_2$ and $^{12}C^{16}O_2$. Mol Phys 2002;100:3563–76.
[44] Di Lonardo G, Baldan A, Bramati G, Fusina L. The infrared spectrum of $^{12}C^{13}CH_2$: the bending states up to $v_4 + v_5 = 4$. J Mol Spectrosc 2002;213:57–63.
[45] Herregodts F, Hurtmans D, Vander Auwera J, Herman M. Laser spectroscopy of the $v_1 + 3v_3$ absorption band in $^{12}C_2H_2$. I: pressure broadening and absolute line intensity measurements. J Chem Phys 1999;111:7954–60.
[46] Herregodts F, Huet T, Vander Auwera J. Absolute line intensities in the v_1+3v_3 band of $^{12}C_2H_2$ by laser photoacoustic spectroscopy and Fourier transform spectroscopy, Mol Phys. submitted.
[47] El Hachtouki R, Vander Auwera J. Absolute line intensities in acetylene: the 1.5-μm region. J Mol Spectrosc 2002;216:355–62.
[48] Pine AS, Looney JP. Decoupling in the line mixing of acetylene infrared Q branches. J Chem Phys 1990;93:6942–53.
[49] Pine AS. Self-, N_2-, and Ar-broadening and line mixing in HCN and C_2H_2. JQSRT 1993;50:149–66.
[50] Blanquet G, Walrand J, Bouanich JP. Line-mixing effects in He- and N_2- broadened Q branches of C_2H_2 at low temperatures. J Mol Spectrosc 2001;210:1–7.
[51] Rothman LS, Gamache RR, Tipping RH, Rinsland CP, Smith MAH, Benner DC, Devi VM, Flaud JM, Camy-Peyret C, Perrin A, Goldman A, Massie ST, Brown LR, Toth RA. The HITRAN molecular database: editions of 1991 and 1992. JQSRT 1992;48:46–507.
[52] Palmer AS, Mickelson ME, Rao KN. Investigations of several infrared bands of $^{12}C_2H_2$ and studies of the effects of vibrational rotational interactions. J Mol Spectrosc 1972;44:131–44.

[53] Podolske JR, Loewenstein M, Varanasi P. Diode laser line strength measurements of the $(\nu_4+\nu_5)^0$ band of $^{12}C_2H_2$. J Mol Spectrosc 1984;107:241–9.
[54] Kabbadj Y, Herman M, Di Lonardo G, Fusina L, Johns JWC. The bending energy levels of C_2H_2. J Mol Spectrosc 1991;150:535–65.
[55] Lambot D, Blanquet G, Bouanich JP. Diode laser measurements of collisional broadening in the ν_5 band of C_2H_2 perturbed by O_2 and N_2. J Mol Spectrosc 1989;136:86–92.
[56] Bouanich JP, Lambot D, Blanquet G, Walrand J. N_2- and O_2-broadening coefficients of C_2H_2 IR lines. J Mol Spectrosc 1990;140:195–213.
[57] Bouanich JP, Blanquet G, Populaire JC, Walrand J. Nitrogen broadening of acetylene lines in the ν_5 band at low temperature. J Mol Spectrosc 1998;190:7–14.
[58] Bouanich JP, Blanquet G, Walrand J. Oxygen broadening of acetylene lines in the ν_5 band at low temperature. J Mol Spectrosc 1999;194:269–77.
[59] Babay A, Ibrahimi M, Lemaire V, Lemoine B, Rohart F, Bouanich JP. Line frequency shifting in the ν_5 band of C_2H_2. JQSRT 1998;59:195–202.
[60] Sun C, Varanasi P. Private communication.
[61] Plateaux JJ, Régalia L, Boussin C, Barbe A. Multispectrum fitting technique for data recorded by Fourier transform spectrometer. Application to N_2O and CH_3D. JQSRT 2001;68:507–20.
[62] Jacquemart D, Mandin JY, Dana V, Picqué N, Guelachvili G. A multispectrum fitting procedure to deduce molecular line parameters. Application to the 3-0 band of $^{12}C^{16}O$. Eur Phys J D 2001;14:55–69.
[63] Plateaux JJ, Barbe A, Delahaigue A. Reims high resolution Fourier transform spectrometer. Data reduction for ozone. Spectrochim Acta 1995;51A:1153–69.
[64] Régalia L. Mesures à l'aide d'un spectromètre par transformation de Fourier, des intensités et coefficients d'élargissement de molécules d'intérêt atmosphérique. Étude des précisions: application à N_2O, H_2O, O_3. Thèse, Université de Reims-Champagne-Ardenne, Reims, France, 1996.
[65] Gamache RR, Hawkins RL, Rothman LS. Total internal partition sums in the temperature range 70–3000 K: atmospheric linear molecules. J Mol Spectrosc 1990;142:205–19.
[66] Gamache RR, Kennedy S, Hawkins RL, Rothman LS. Total internal partition sums for molecules in the terrestrial atmosphere. J Mol Struct 2000;517-8:407–25.
[67] Weber M, Blass WE, Nadler S, Halsey GW, Maguire WC, Hillman JJ. ℓ-Resonance effects in C_2H_2 near 13.7 μm. Part II: the two-quantum hotbands. Spectrochim Acta 1993;49A:1659–81.
[68] Sinclair PM, Duggan P, Berman R, Drummond JR, May AD. Line broadening in the fundamental band of CO in CO–He and CO–Ar mixtures. J Mol Spectrosc 1998;191:258–64.